Colloids and Surfaces B: Biointerfaces 265 (2026) 115741

Contents lists available at ScienceDirect

Colloids and Surfaces B: Biointerfaces

journal homepage: www.elsevier.com/locate/colsurfb

Agarose gelation beyond equilibrium through distributed kinetic pathways and apparent thermodynamic signatures

Antonio de Nigris [a], Francesco Lopez [b], Emiliano Fratini [c], Lorenzo Mio [e], Ivan Donati [d], Pasquale Sacco [d], Luigi Ambrosone [a,*]

[a] Department of Medicine and Health Sciences, University of Molise, Via De Sanctis, Campobasso, 86100, Italy
[b] Department of Agricultural, Environmental and Food Sciences, University of Molise, Via De Sanctis, Campobasso, 86100, Italy
[c] Department of Chemistry "Ugo Schiff" and CSGI, University of Florence, Via della lastruccia, 3, Florence, 50019, Italy
[d] Department of Life Sciences, University of Trieste, Via Licio Giorgieri, 5, Trieste, 34127, Italy
[e] Department of Medicine, Surgery and Health Sciences, University of Trieste, I-34129, Trieste, Italy

ARTICLE INFO

Keywords:
Agarose gelation
Differential scanning calorimetry (DSC)
Distributed kinetics
Non-equilibrium gelation
Stochastic interpretation

ABSTRACT

The gelation of agarose in aqueous solution is studied by differential scanning calorimetry (DSC) under non-isothermal cooling at different rates. The thermograms show a clear exothermic peak whose position and shape depend on the cooling rate, highlighting the coupling between the imposed thermal protocol and the intrinsic timescales of network formation. The sol–gel transition is described through a temperature- and rate-dependent degree of transformation, defined as the normalized fraction of exchanged enthalpy. This model-free parameter yields sigmoidal conversion curves that progressively shift and distort at higher cooling rates, indicating a deviation from quasi-equilibrium conditions. Extrapolation to zero cooling rate identifies a unique gelation temperature, independent of protocol and conversion level, thereby providing an operational gel point. The derivative of the conversion yields a kinetic profile whose broadening at high rates reflects cooperative, distributed, non-equilibrium gelation dynamics.

1. Introduction

Agarose is a marine-derived, essentially uncharged polysaccharide that is often used as a model biopolymer in gelation studies. Agarose is obtained from marine red algae and is chemically composed of repeating units of 3-linked β-D-galactopyranose and 4-linked 3,6-anhydro-α-L-galactopyranose [1]. Agarose is a prototypical physical gel former and has long served as a model system for investigating sol–gel transitions in polysaccharide solutions [2]. Upon cooling from the sol state, agarose undergoes a thermoreversible gelation process [3] driven by the formation of ordered junction zones [4] and their progressive organization into a percolating network stabilized by non-covalent interactions. Despite its apparent simplicity, agarose gelation is a complex, multiscale phenomenon involving molecular ordering, aggregation [5] and network growth [6], whose underlying mechanisms remain the subject of active investigation [7,8]. Upon cooling, agarose solution undergoes a rapid and often poorly controlled sol–gel transition, forming a three-dimensional network, due to its molecular structure and physico-chemical properties [9–13]. During gelation under cooling, the single chains first associate via hydrogen bonds to form double helices [14]. Further cooling leads to aggregation of these double helices [13]. Although agarose-, and more broadly, agar-based gels have been extensively studied in the past 30 years, the gelation mechanism still remains a matter of debate [11,15–19]. The most widely accepted mechanism proposed in the literature for agarose gelation is a two-step process: first, the connection of the randomly distributed coils by hydrogen bonds to form a double-helical association, followed by the aggregation of the double helices to form a tight three-dimensional network.

Polymer gels are a class of materials that have attracted considerable interest because of their versatility, soft-structure, and flexibility. Based on their properties, such kind of molecules can be used in a wide range of applications such as food industry, agriculture and biomedicine [20]. In this context, Differential scanning calorimetry (DSC) has been widely employed to characterize agarose gelation, providing access to characteristic temperatures and thermal signatures associated with junction zone formation [14]. Traditionally, these calorimetric features have often been interpreted within a thermodynamic framework, implicitly assuming quasi-equilibrium conditions during the sol–gel transition. However, a growing body of experimental evidence demonstrates that agarose gelation is inherently

* Corresponding author.
E-mail address: ambroson@unimol.it (L. Ambrosone).

https://doi.org/10.1016/j.colsurfb.2026.115741
Received 11 March 2026; Received in revised form 12 April 2026; Accepted 22 April 2026
Available online 24 April 2026

path-dependent: the shape, position, and width of the calorimetric transition are strongly affected by concentration, thermal history, and, crucially, by the applied heating or cooling rate. The pronounced dependence of DSC curves on the scanning rate (β) highlights the presence of kinetic constraints that govern the transformation pathway. Variable-rate calorimetric experiments reveal systematic shifts of characteristic temperatures, significant changes in peak asymmetry and broadening, and the emergence of rate-dependent transition widths. These observations indicate that the calorimetric signal does not represent a simple equilibrium phase transition, but rather reflects the collective outcome of kinetically controlled processes occurring over a broad range of length and time scales. In this context, the interpretation of calorimetric data in terms of a temperature-dependent degree of transformation, $\theta(T)$, provides a powerful and model-independent description of the gelation process. Under non-isothermal conditions, $\theta(T)$ captures the progressive conversion from the sol-like to the gel-like state, while its temperature derivative naturally reflects the distribution of transformation events along the thermal pathway. The resulting calorimetric profiles thus encode information on the kinetics of network formation, rather than on a well-defined thermodynamic potential. In this work, we investigate agarose gelation by means of variable-rate differential scanning calorimetry, adopting a kinetic and probabilistic perspective explicitly tailored to non-equilibrium conditions. By analyzing the evolution of $\theta(T)$, its derivative, and the associated transition widths as functions of the scanning rate, we show that agarose gelation is governed by distributed and cooperative kinetic pathways. This approach provides a unified framework for interpreting calorimetric signatures without invoking equilibrium assumptions, offering new insight into the fundamental mechanisms underlying physical gelation in polysaccharide systems.

2. Materials and methods

2.1. Materials

Agarose for electrophoresis (EP) (code EMR920500) was purchased from (Euroclone, Italy). The physicochemical characteristics of the agarose used in the present study have been previously described [21], and are as follows: residual content of agaropectins (in terms of ashes) = 0.6% w/w. Gelling temperature = 34 °C, determined with [agarose] = 1.5% w/V. The shear viscosity of the agarose solution (1.5% w/V) at 60 °C was measured using rotational viscometry, yielding a value of 14 mPa· s. Total methylation = 7.4% was determined by ^{1}H- and ^{13}C-HSQC.

2.2. Agarose solution preparation

A 0.15% (w/w) agarose solution was prepared by dispersing the polymer in deionized water. Solutions were then stirred for 1 h and autoclaved at 121 °C for 15 min. After the treatment, all the solutions appeared homogeneous.

2.3. DSC analysis

The DSC investigation was conducted using a Mettler Toledo DSC 5+ instrument with 136 thermocouples, 2 integrated resistors and a ceramic MMS 1 sensor, operating in the temperature range 25 °C – 600 °C with 40 μl aluminum crucibles sealed with lids. The instrument has a sampling frequency of 50 Hz, a temperature accuracy ± 0.2 K, a temperature precision of ± 0.2 K, and it is operated using STAR^{e} software. The freshly prepared solutions in glass vials were autoclaved at high temperatures, then kept under agitation for 20 min and stored at room temperature. Before DSC measurements, the vials were placed in an oven at 60 °C. Then, 20 μl of the solution were poured into an aluminum crucible (volume of 40 μl) and sealed with a pierced lid. The crucible was inserted in the DSC thermostatted housing chamber kept at 60 °C. After a brief equilibration period, the instrument automatically started the measurement. The system, although diluted, remained in the gel phase due to the hysteresis effect. Moreover, a test conducted on a sample diluted to 0.15% (w/w) in the temperature range 90–25 °C showed no difference compared to the sample analyzed over the range 60–25 °C. DSC experiments were conducted by setting temperature ramps in the range of 60–25 °C, using the following cooling rates: 1, 3, 5, 7 and 10 °C min^{-1}.

3. Results and discussion

Fig. 1 shows the DSC thermograms obtained at different cooling rates. All curves exhibit a pronounced exothermic event associated with the formation of the agarose gel network, in accordance with the literature [14]. The position of this event systematically shifts toward lower temperatures as the cooling rate β is reduced. This behavior immediately indicates a strong interplay between the imposed thermal protocol and the intrinsic timescales governing the gelation process. As a first phenomenological approximation, the sol–gel transition is described in terms of the coexistence of two macroscopic states, conventionally referred to as sol and gel, i.e.

$$\mathrm{Sol} \rightleftharpoons \mathrm{Gel}$$

Within this framework, the extent of the transition is quantified by the experimental parameter θ, defined as the fraction of the total heat exchanged up to temperature T. Since the calorimetric response depends on the applied cooling rate, this quantity is, in general, a function of both temperature and scan rate, and is defined as

$$\theta(T,\beta) = \frac{\int_{T}^{T_{max}} Q(T',\beta)dT'}{\int_{T_{min}}^{T_{max}} Q(T',\beta)dT'} \tag{1}$$

where $Q(T,\beta)$ is the heat flux, normalized to the sample mass (W·g^{-1}), exchanged between the sample and the reference as a function of temperature and cooling rate.

By construction, $\theta = 0$ corresponds to the initial sol state where no gelation enthalpy has been released, while $\theta = 1$ represents the fully developed gel state. Intermediate values of θ provide a normalized measure of the progress of the gelation process in terms of released enthalpy. The θ values calculated from the thermograms of Fig. 1 are shown in Fig. 2(a). For each cooling rate, $\theta(T,\beta)$ exhibits a sigmoidal temperature dependence, characteristic of a progressive transformation occurring over a finite temperature interval. The sigmoidal shape reflects an initially slow increase of θ, followed by a rapid growth region and a final saturation, consistent with a cooperative process involving multiple interacting units. As β increases, the sigmoidal curves shift toward higher temperatures and progressively lose symmetry, indicating an increasing decoupling between the imposed cooling rate and the intrinsic relaxation processes associated with network formation. Thus, although the transition can be formally represented as a two-state process at the macroscopic level, the observed sigmoidal behavior clearly points to a cooperative transformation rather than an ideal two-state equilibrium. A closer inspection of the initial portion of the curves reveals no evidence of a measurable induction period within the experimental resolution. The degree of transformation increases continuously from the earliest stages of cooling, without any detectable plateau at low θ. This observation suggests that gelation does not proceed via a nucleation-controlled mechanism characterized by a distinct induction stage, but rather through a continuous and cooperative process in which structural rearrangements progressively develop over the entire temperature range. In order to quantify the degree of cooperativity without invoking a specific equilibrium model, we introduce a model-free descriptor based on the width of the sigmoidal $\theta(T,\beta)$ curves. Since the degree of transformation $\theta(T)$ is defined as a monotonically decreasing function of temperature, with $\theta \approx 0$ in the sol state and $\theta \approx 1$ in the gel state, the characteristic temperature width of the transition is defined as

$$\Delta T = T(\theta = 0.1,\beta) - T(\theta = 0.9,\beta)$$

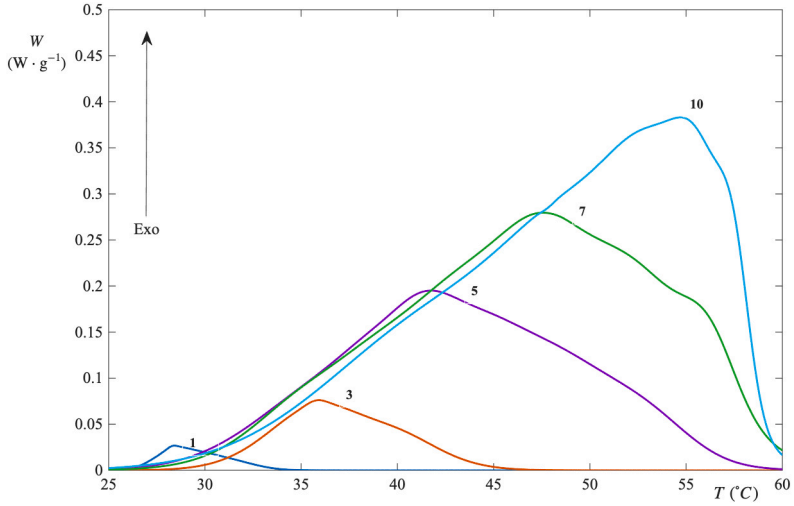

Fig. 1. DSC thermograms of the agarose solution recorded at various cooling rates. Each exothermic peak corresponds to the gelation process labeled according to its specific cooling rate in units K·min^{-1}.

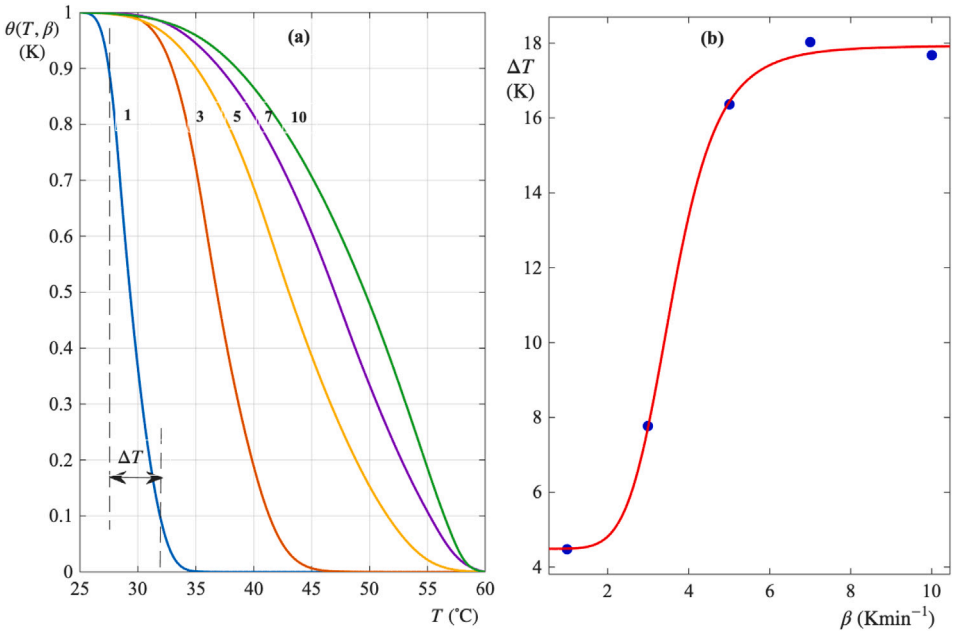

Fig. 2. (a) Fraction of total heat exchange $\theta(T,\beta)$ displaying a sigmoidal profile, from which the characteristic temperature interval ΔT of the process is extracted. The numbers on the curves represent the cooling rate in K·min^{-1}. (b) The calculated ΔT values plotted as a function of cooling rate. The data are well described by a four parameter sigmoidal fit, highlighting the systematic dependence ΔT on the imposed cooling conditions.

which represents the positive temperature interval over which the main fraction of the gelation process takes place. As shown in Fig. 2(a), this parameter provides a direct measure of how sharply the gel–sol transition is distributed along the temperature axis. Indeed, a narrow ΔT corresponds to a highly cooperative transformation, whereas a broader ΔT reflects a more progressive, weakly cooperative process. Fig. 2(b) shows that the $\Delta T(\beta)$ is well described by a sigmoidal function of the form

$$\Delta T(\beta) = a - \frac{b}{1+\left(\frac{\beta}{c}\right)^{d}} \qquad R^2 = 0.9991; \quad RMSE = 0.4 \tag{2}$$

with $a = 17.9$, $b = 13.4$, $c = 3.6$ and $d = 6.3$.

At low β, ΔT approaches a minimum value, reflecting highly synchronized structural rearrangements under near quasi-equilibrium conditions. In an intermediate range of cooling rates, ΔT increases rapidly, signaling a progressive decoupling of elementary ordering events. At high β, ΔT reaches a plateau, indicating that the transformation is fully kinetically limited and that further increases in the cooling rate do not qualitatively alter the nature of the gelation process.

This aspect was further investigated by determining, for fixed values of θ, the corresponding temperatures at different cooling rates. For each chosen θ, the temperature values obtained at different β are displayed in Fig. 3. In all cases, the temperature dependence on β is well fitted by a second-degree polynomial. Remarkably, extrapolation to the limit $\beta \to 0$ leads all curves to converge to the same temperature, $T = (24.8 \pm 0.2)$ °C. In other words, there exists a temperature such that

$$\lim_{\beta \to 0} T(\theta,\beta) = T_g \tag{3}$$

independent of both the cooling rate and the gel fraction θ. This limiting value is therefore identified as the intrinsic gelation temperature of

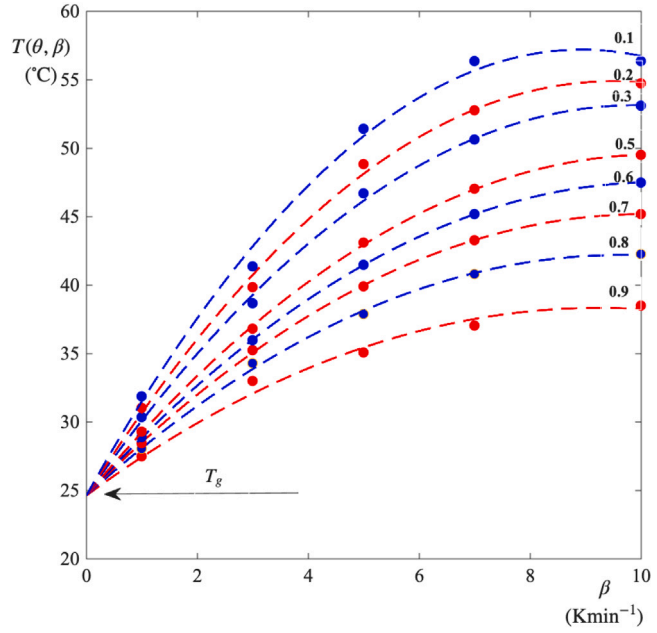

Fig. 3. Temperature at fixed θ as a function of the cooling rate β. Each curve corresponds to a different prescribed value of θ, as indicated along the respective line. A second order polynomial fit of the data points shows that all curves converge, in the limit $\beta \to 0$, to the same temperature T_g.

the system, free from kinetic distortions imposed by the experimental protocol. In Ref. [21], a gelation temperature of 34 °C was reported using a hard-shaking method. However, it is important to note that the agarose concentration employed in that study was 1.5% (w/V), approximately one order of magnitude higher than in the present case. Seminal work by Mohammed *et al.* [22], as well as more recent studies on the role of mechanical stimulation in agarose gelation [11], clearly demonstrate that T_g scales with polymer concentration. Therefore, direct comparison of T_g values obtained at substantially different concentrations should be made with caution.

Since the points chosen for verifying Eq. (3) are arbitrary, it follows that there is no limiting distribution. Mathematically, this means that the function $\theta(T,0)$ degenerates into a step function, i.e.

$$\lim_{\beta\to 0}\theta(T,\beta) = \begin{cases} 0 & T > T_g \\ 1 & T < T_g \end{cases}$$

which is written as

$$\lim_{\beta\to 0}\theta(T,\beta) = \mathcal{H}(T - T_g) \tag{4}$$

where $\mathcal{H}(x)$ is the Heaviside function [23]. Thus, within the two–state phenomenological description introduced above, the function $\theta(T,\beta)$ can be regarded as a cumulative distribution function describing the probability that a given fraction of the system has undergone gelation upon cooling down to temperature T. Consequently, its temperature derivative

$$P(T,\beta) = \frac{d\theta}{dT} \tag{5}$$

defines a probability density function that quantifies how gelation events are distributed along the temperature axis. Physically, $P(T,\beta)dT$ represents the probability that an infinitesimal fraction of the system undergoes gelation within the temperature interval $[T, T+dT]$ under a given cooling rate. The existence of a well-defined maximum in $P(T,\beta)$ indicates the temperature at which gelation events are statistically most probable. Importantly, this temperature does not correspond to a thermodynamic transition point, but rather reflects the most favorable balance between thermodynamic driving force and kinetic accessibility along the imposed thermal pathway. Under linear cooling conditions, where the temperature is related to time through

$$T(t) = T_0 + \beta t \tag{6}$$

the stochastic description in temperature space can be directly mapped onto the time domain. Indeed, using this relation, the rate of gelation is given by

$$\frac{d\theta}{dt} = \beta\frac{d\theta}{dT} = \beta P(T,\beta) \tag{7}$$

Accordingly, the probability density $P(T,\beta)$ is proportional to the instantaneous gelation rate, and the maximum of $-d\theta/dT$ coincides with the maximum transformation rate in time. Since the cooling rate β acts only as a scaling factor, the position of the maximum remains unchanged, while its magnitude directly reflects the kinetics of the process. Fig. 4 shows the systematic shift of the probability density peak toward higher temperatures with increasing β, together with its progressive broadening and loss of symmetry, provides clear evidence that agarose gelation proceeds through a distributed and cooperative kinetic process. At low cooling rates, the narrow and nearly symmetric probability distribution indicates that gelation events are highly synchronized, consistent with conditions approaching quasi-equilibrium. As the cooling rate increases, the distribution broadens and becomes increasingly asymmetric, reflecting a widening spectrum of characteristic timescales associated with helix formation, aggregation, and network rearrangement.

The conservation of the total probability,

$$\int_{-\infty}^{+\infty}\frac{d\theta}{dT}dT = 1 \tag{8}$$

ensures that the overall extent of the transformation remains unchanged, even though its distribution along the temperature axis varies significantly with β. Thus, changes in peak height and width do not reflect variations in the amount of gel formed, but rather how the gelation process is temporally and thermally distributed. Furthermore, the stochastic description naturally rationalizes the observed increase of the sigmoidal width ΔT with increasing cooling rate. The parameter ΔT directly measures the spread of the underlying probability distribution and therefore provides a model-free quantification of the degree of cooperativity of the process. Narrow distributions correspond to strongly cooperative transformations, while broader distributions indicate progressively weaker cooperativity and enhanced kinetic heterogeneity. At the lowest cooling rate, the derivative peak is narrow, intense, and nearly symmetric, indicating that a large fraction of the transformation occurs within a limited temperature interval and is characterized by a relatively narrow distribution of kinetic pathways. This behavior is consistent with conditions approaching quasi-equilibrium, where the cooperative ordering of agarose chains proceeds in a concerted manner. As the cooling rate increases, the derivative peaks progressively broaden and their maximum intensity decreases, reflecting an increasing dispersion of characteristic timescales and a reduction in the instantaneous transformation rate. Under these conditions, nucleation, growth, and structural reorganization are no longer synchronized but occur over distinct temperature intervals, leading to asymmetric derivative profiles. Taken together, the sigmoidal temperature dependence of θ and the systematic evolution of $d\theta/dT$ with β indicate that the calorimetric signal primarily reflects the kinetics of structural evolution rather than a simple equilibrium phase transition. The kinetic behavior evidenced by the calorimetric data is most naturally interpreted within the framework of distributed kinetics. In such systems, the macroscopic transformation does not proceed through a single characteristic timescale, but rather emerges from a population of elementary events characterized by a broad distribution of activation barriers and relaxation times. Under non-isothermal conditions, the imposed cooling rate acts as an external constraint that selectively activates or suppresses subsets of these events, leading to protocol-dependent rate profiles and transformation widths. This perspective provides a natural explanation

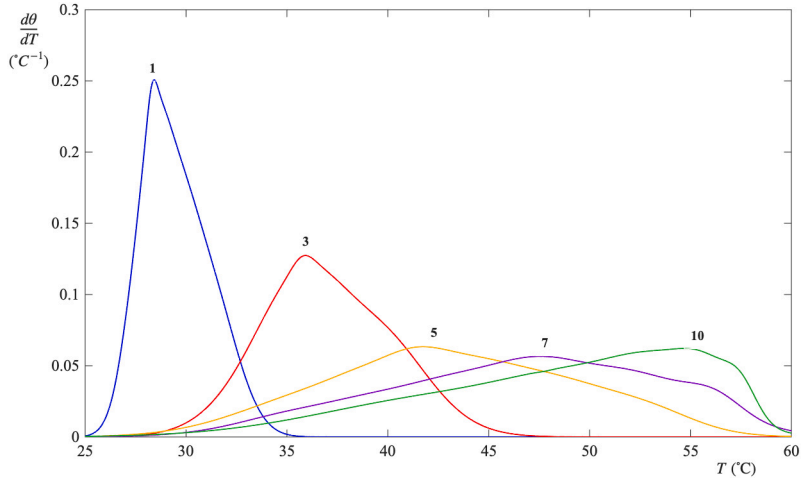

Fig. 4. Derivative curves $d\theta/dT$ plotted as a function of temperature for different cooling rates β. Each curve is labeled with its corresponding β value. The maxima of the curves identify the temperatures at which the gelation event is statistically most probable.

for the observed broadening and asymmetry of the rate peaks, as well as for the sigmoidal dependence of ΔT on the cooling rate. From this viewpoint, agarose gelation can be regarded as a stochastic, cooperative process, in which network formation results from the collective evolution of interacting structural units rather than from a sequence of independent elementary steps. The model-free kinetic descriptors adopted in this work are therefore not merely convenient, but conceptually appropriate, as they capture the emergent nature of the transformation without imposing a predefined microscopic mechanism. The rate dependence of the transition width shown in Fig. 4 can also be discussed in light of the structural scenario proposed by Mohammed *et al.* [22], who suggested that the helix length required for stable association increases with temperature and that slower cooling favors the formation of longer helices, thereby enhancing helix–helix aggregation. Within the present probabilistic framework, the narrowing of the distribution $d\theta/dT$ observed at low cooling rates can be interpreted as a signature of increased cooperativity in the gelation process. A sharper distribution implies that a large fraction of the system transforms within a restricted temperature interval, consistent with a more collective and correlated assembly of junction zones. In contrast, rapid quenching broadens the probability distribution and increases the transition width ΔT, indicating that gelation events are distributed over a wider temperature range. This behavior is compatible with the formation of shorter or structurally heterogeneous helices that associate less cooperatively, leading to a larger dispersion of local transformation conditions. In this sense, the cooperativity inferred from calorimetric analysis may reflect variations in helix length, junction number, and aggregation extent controlled by the cooling rate. Although DSC does not provide direct structural information, the systematic evolution of ΔT and of the peak symmetry with cooling rate suggests that the apparent thermodynamic signatures arise from changes in the collective organization of helices. The probabilistic description adopted here therefore complements the structural interpretation of Mohammed *et al.* [22] by linking helix growth and aggregation to a measurable kinetic broadening or sharpening of the transformation pathway.

Finally, it is worth emphasizing that the present results cannot be consistently interpreted within conventional isoconversional [24] frameworks, such as the Friedman's method [25–27]. These approaches rely on the assumption of a separable rate law, in which the transformation rate can be expressed as the product of a temperature-dependent term and a conversion-dependent function, as well as on the existence of a unique activation energy governing the process.

However, the analysis reported here clearly shows that agarose gelation proceeds through distributed and cooperative kinetic pathways, whose relative contributions depend on the imposed cooling rate. In this context, the quantity $d\theta/dT$ is more appropriately interpreted as a probability density of transformation events rather than as the rate of a single elementary process.

Consequently, the apparent activation energies [28,29] that would be obtained from isoconversional methods would not correspond to intrinsic energetic barriers, but rather to effective parameters reflecting the convolution of multiple processes with different characteristic timescales. For this reason, such methods are not expected to provide physically meaningful insight into the gelation mechanism in the present system.

A similar limitation applies to isothermal approaches. Due to the distributed and cooperative nature of agarose gelation, the transformation cannot be described in terms of a single activation energy or a well-defined kinetic pathway. As a result, isothermal measurements would yield apparent characteristic times that depend on the thermal history and on the initial structural state, rather than intrinsic thermodynamic or kinetic parameters.

4. Robustness and reliability of the reconstructed thermal response

The robustness of the reconstructed thermal response was assessed through the combined analysis of the $T(\theta, \beta)$ surface and the associated confidence bounds obtained via propagation of instrumental uncertainties [30,31]. Although replicate measurements were not available for each cooling rate, the intrinsic reproducibility of DSC experiments and the controlled magnitude of the instrumental error ($\pm 0.2\,^{\circ}$C on peak temperature and 2%–3% on enthalpy) allow for a reliable evaluation of the consistency of the results. This combined analysis is summarized in Fig. 5. Panel (a) shows the temperature difference $\Delta T(\theta)$ between two representative cooling rates, together with the propagated uncertainty band. Over most of the conversion range, the confidence interval appears visually compressed due to its small magnitude relative to the overall temperature scale, giving the impression of nearly overlapping curves. However, the inset reveals that the confidence band is finite and well-defined, particularly in the intermediate conversion region. This zoomed view highlights that the uncertainty remains on the order of the instrumental resolution and is therefore small but not negligible. Importantly, within the central region of the transformation, the temperature difference exceeds the confidence interval, indicating that the observed deviation between cooling rates is not attributable to experimental uncertainty but reflects a genuine kinetic effect. Outside the transition region, the temperature difference remains within the confidence bounds, indicating that the system response is effectively independent of the cooling rate and highly consistent. Overall, the

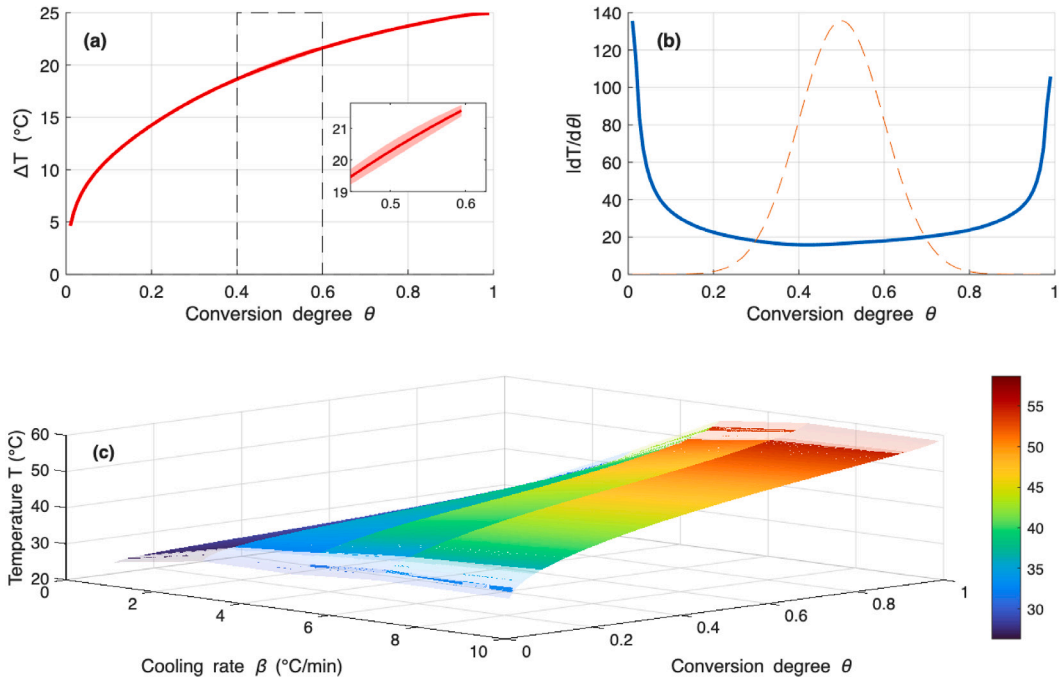

Fig. 5. Combined representation of the reconstructed thermal response. (a) Temperature difference between cooling rates with uncertainty band. The inset shows that the uncertainty is nonzero. (b) Derivative profile identifying the gelation region. (c) Surface $T(\theta, \beta)$ with confidence bounds. The results highlight a highly consistent behavior outside the transition region and a localized increase in sensitivity and uncertainty during gelation, indicating a cooperative and rate-dependent transformation.

analysis confirms that the propagated uncertainty is tightly controlled and that the reconstructed thermal response is robust, with significant rate dependence confined to the gelation domain. Panel (b) reports the absolute derivative $|dT/d\theta|$, which quantifies the sensitivity of temperature to the degree of conversion. A pronounced peak is observed in the intermediate θ range, identifying the gelation region as the zone of maximum variation of the DSC signal. Notably, this region coincides with the maximum of the propagated uncertainty, indicating that the system is most sensitive to experimental perturbations during the phase transition. This behavior is characteristic of a cooperative process, where the transformation occurs over a finite interval rather than at a sharply defined point. Panel (c) presents the reconstructed surface $T(\theta, \beta)$ together with its confidence bounds, providing a global representation of the thermal pathway across different cooling rates. The surface exhibits a clear dependence on β, reflecting the kinetic nature of the process. The confidence envelope remains negligible in the regions corresponding to low and high conversion, indicating a high level of reliability and stability of the reconstructed data. In contrast, the uncertainty increases in the central region, where the transition takes place, highlighting the intrinsic sensitivity of the system during gelation. Overall, the surface confirms that the sol–gel transition is not a single-temperature event but a distributed process in the (θ, β) space, governed by cooperative effects and influenced by the cooling rate. Overall, the results demonstrate that the proposed approach provides a reliable and physically consistent framework for analyzing thermally driven transitions, where experimental uncertainty is well quantified and kinetic effects are clearly distinguishable from measurement variability.

5. Conclusions

A refined thermodynamic-kinetic picture of agarose gelation has been presented, in which the process is interpreted beyond the conventional equilibrium framework. By introducing a monotonic degree of transformation, $\theta(T)$, derived from calorimetric measurements and defined as the fraction of ungelled material, gelation is described as a continuous transition driven by a distribution of microscopic kinetic events rather than by a single, well-defined reaction pathway. Within this framework, the temperature derivative $d\theta/dT$ naturally acquires the meaning of a probability density, reflecting the likelihood that a fraction of the system undergoes gelation within a given temperature interval. The experimentally observed thermal signatures are therefore shown to encode not an equilibrium thermodynamic potential, but the collective outcome of distributed and overlapping kinetic processes. The characteristic width of the transition, quantified through the temperature interval ΔT provides a direct and model-independent measure of the dispersion of these kinetic pathways and of the degree of cooperativity involved in network formation. The dependence of both the transition temperature and its width on the cooling rate further highlights the intrinsically non-equilibrium nature of agarose gelation. In this context, traditional notions such as reaction order or single activation barriers lose their strict applicability, while a stochastic and probabilistic description emerges as a more appropriate and physically meaningful representation of the process. Overall, this approach establishes a unified interpretation of calorimetric, kinetic, and probabilistic aspects of agarose gelation, offering a general framework that can be extended to other physically crosslinked polymer systems characterized by distributed kinetics and pathway-dependent transformations.

CRediT authorship contribution statement

Antonio de Nigris: Software, Formal analysis, Data curation. **Francesco Lopez:** Writing – review & editing, Methodology, Formal analysis. **Emiliano Fratini:** Writing – review & editing, Supervision. **Lorenzo Mio:** Software. **Ivan Donati:** Writing – review & editing, Visualization. **Pasquale Sacco:** Writing – review & editing, Supervision. **Luigi Ambrosone:** Writing – original draft, Methodology, Data curation, Conceptualization.

Declaration of competing interest

The authors declare that they have no known competing financial interests or personal relationships that could have appeared to influence the work reported in this paper.

Acknowledgments

The authors thank the Consorzio Interuniversitario per lo Sviluppo dei Sistemi a Grande Interfase (CSGI) for partial financial support.

Data availability

The data supporting the findings of this study are available from the corresponding author upon reasonable request.

References

[1] P. Zarrintaj, S. Manouchehri, Z. Ahmadi, M.R. Saeb, A.M. Urbanska, D.L. Kaplan, M. Mozafari, Agarose-based biomaterials for tissue engineering, Carbohydr. Polymers 187 (2018) 66–84.
[2] Z. Wang, K. Yang, H. Li, C. Yuan, X. Zhu, H. Huang, Y. Wang, L. Su, Y. Fang, Situ observation of sol–gel transition of agarose aqueous solution by fluorescence measurement, Int. J. Biol. Macromol. 112 (2018) 803–808.
[3] A.S. Ogrenci, O. Pekcan, S. Kara, A.H. Bilge, Mathematical characterization of thermo-reversible phase transitions of agarose gels, J. Macromol. Sci. Part B 57 (2018) 364–376.
[4] M. Trudicova, J. Smilek, M. Kalina, M. Smilkova, K. Adamkova, K. Hrubanova, V. Krzyzanek, P. Sedlacek, Multiscale experimental evaluation of agarose-based semi-interpenetrating polymer network hydrogels as materials with tunable rheological and transport performance, Polymers 12 (2020) 2561.
[5] S.N. Bagriantsev, V.V. Kushnirov, S.W. Liebman, Multiscale experimental evaluation of agarose-based semi-interpenetrating polymer network hydrogels as materials with tunable rheological and transport performance, Methods Enzymol. 412 (2006) 33–48.
[6] E. Amici, A.H. Clark, V. Normand, N.B. Johnson, Interpenetrating network formation in Gellan- agarose gel composites, Biomacromolecules 1 (2000) 721–729.
[7] N. Watase, K. Nishinari, T. Hatakeyama, DSC study on properties of water in concentrated agarose gels, Food Hydrocolloids 2 (1988) 427–438.
[8] E. Fernández, D. López, C. Mijangos, M. Duskova-Smrckova, M. Ilavsky, K. Dusek, Rheological and thermal properties of agarose aqueous solutions and hydrogels, J Polym. Sci. Part B: Polym. Phys. 46 (2008) 322–328.
[9] S. Arnott, A.S.W.E. Fulmer, W.E. Scott, I.C.M. Dea, R. Moorhouse, D.A. Rees, The agarose double helix and its function in agarose gel structure, J. Mol. Biol. 90 (1974) 269–284.
[10] M. Ghebremedhin, S. Seiffert, T.A. Vilgis, Physics of agarose fluid gels: Rheological properties and microstructure, Curr. Res. Food Sci. 4 (2021) 436–448.
[11] L. Mio, F. Piazza, M. Abrami, M. Conti, F. Lopez, E. Fratini, M. Grassi, F. Brun, I. Donati, P. Sacco, Effect of anions, concentration and mechanical stimulation on the gelation of agarose, Int. J. Biiol. Macromol. (2026) 150233.
[12] D. Nordqvist, T.A. Vilgis, Rheological study of the gelation process of agarose-based solutions, Food Biophys. 6 (2011) 450–460.
[13] N. Russ, B.I. Zielbauer, K. Koynov, T.A. Vilgis, Influence of nongelling hydrocolloids on the gelation of agarose, Biomacromolecules 14 (2013) 4116–4124.
[14] T. Singh, R. Meena, A. Kumar, Effect of sodium sulfate on the gelling behavior of agarose and water structure inside the gel networks, J. Phys. Chem. B 113 (2009) 2519–2525.
[15] H. Jung, L.C. Geonzon, W.B. Yoon, S. Matsukawa, Change of network structure in agarose solution during gelation studied by multiple particle tracking and NMR measurements, Food Hydrocolloids 141 (2023) 108740.
[16] A. Rüther, A. Forget, A. Roy, C. Carballo, F. Mießmer, R. Dukor, L. Nafie, C. Johannessen, V. Shastri, S. Lüdeke, Unravelling a direct role for polysaccharide β-strands in the higher order structure of physical hydrogels, Angew. Chem. 129 (2017) 4674–4678.
[17] M. Martínez-Sanz, A. Ström, P. Lopez-Sanchez, S. Knutsen, S. Ballance, H. Zobel, A. Sokolova, E. Gilbert, A. López-Rubio, Advanced structural characterisation of agar-based hydrogels: rheological and small angle scattering studies, Carbohydr. Polymers 236 (2020) 115655.
[18] J. Xiong, J. Narayanan, X. Liu, T. Chong, S. Chen, T. Chung, Topology evolution and gelation mechanism of agarose gel, J. Phys. Chem. B 109 (2005) 5638–5643.
[19] B. Dai, S. Matsukawa, NMR studies of the gelation mechanism and molecular dynamics in agar solutions, Food Hydrocoll. 26 (2012) 181–186.
[20] M. Chelu, A.M. Musuc, Polymer gels: classification and recent developments in biomedical applications, Gels 9 (2023) 161.
[21] F. Piazza, P. Sacco, E. Marsich, G. Baj, F. Brun, F. Asaro, G. Grassi, M. Grassi, I. Donati, Cell activities on viscoelastic substrates show an elastic energy threshold and correlate with the linear elastic energy loss in the strain-softening region, Adv. Funct. Mater. 33 (2023) 2307224.
[22] Z.H. Mohammed, M.W.N. Hember, R.K. Richardson, E.R. Morris, Kinetic and equilibrium processes in the formation and melting of agarose gels, Carbohydr. Polymers 36 (1998) 15–26.
[23] J. Venetis, An analytic exact form of heaviside step function, Adv. Appl. Discrete Math. 22 (2019) 153–159.
[24] N. Sbirrazzuoli, Isoconversional methods: fundamentals and applications, Macromol. Chem. Phys. 208 (2007) 1592–1592.
[25] H.L. Friedman, Kinetics of thermal degradation of char-forming plastics from thermogravimetry. application to a phenolic plastic, J. Polym. Sci. Part C 6 (1964) 183–195.
[26] S. Vyazovkin, A.K. Burnham, J.M. Criado, L.A. Pérez-Maqueda, C. Popescu, N. Sbirrazzuoli, ICTAC kinetics committee recommendations for performing kinetic computations on thermal analysis data, Thermochim. Acta 520 (2011) 1–19.
[27] S. Vyazovkin, Modern isoconversional kinetics: from misconceptions to advance, Thermochim. Acta 688 (2020) 178597.
[28] S. Vyazovkin, Evaluation of activation energy of thermally stimulated solid-state reactions under arbitrary variation of temperature, J. Comput. Chem. 18 (1997) 393–402.
[29] G. Bufalo, L. Ambrosone, Method for determining the activation energy distribution function of complex reactions by sieving and thermogravimetric measurements, J. Phys. Chem. B 120 (2015) 244–249.
[30] T.-C. Lin, H.-H. Chen, K.-S. Chen, Y.-P. Chen, S.-H. Chang, Decision-making model of performance evaluation matrix based on upper confidence limits, Mathematics 11 (2023) 3499.
[31] P. Kaftan, J. Mayr, F. Porquez, K. Pomodoro, D. Trombert, K. Wegener, M. Bambach, Reducing thermal errors with confidence: uncertainty-based compensation for precision machine tools, CIRP J. Manuf. Sci. Technol. 61 (2025) 400–409.